applied sciences

MDPI

Article

Sensitivity Analysis of Numerical Coherency Model for Rock Sites

Dongyeon Lee [1], Yonghee Lee [2], Hak-Sung Kim [2], Jeong-Seon Park [2] and Duhee Park [1,*]

[1] Department of Civil and Environmental Engineering, Hanyang University, Seoul 04763, Republic of Korea; dylee9320@hanyang.ac.kr
[2] Central Research Institute, Korea Hydro & Nuclear Power Co., Ltd., Daejeon 34101, Republic of Korea; dragon202@khnp.co.kr (Y.L.); haksung.kim@khnp.co.kr (H.-S.K.); jpark617@khnp.co.kr (J.-S.P.)
* Correspondence: dpark@hanyang.ac.kr; Tel.: +82-2-2220-0322

Abstract: Characterization of ground motion incoherency can significantly reduce the seismic load imposed on large scale infrastructures. Because of difficulties in developing an empirical coherency function from a site-specific dense array, it is seldom used in practice. A number of studies used numerical simulations to develop generic coherency models. However, they have only been developed for idealized profiles. A comprehensive parametric study evaluating the effect of various parameters influencing the calculated coherency function has not yet been performed. We utilized the measured shear wave velocity (V_s) profile at Pinyon Flat, located in California, to perform a suite of time history analyses. This site was selected because the empirical coherency function developed here has been used as a reference model for rock sites. We performed several sensitivity studies investigating the effect of both the site spatial variability and numerical analysis parameters in order to provide a guideline for developing a coherency model from numerical simulations. The outputs were compared against the empirical coherency model to better illustrate the importance of the parameters. The coefficient of variation (CV) of V_s was revealed to be the primary parameter influencing the calculated plane-wave coherency, whereas the correlation length (CL) has a secondary influence. Site-specific convergence analyses should be performed to determine the optimum numerical parameter, including the number of analyses and depth of numerical model. Considering the importance of CV and V_s, it is recommended to perform field tests to determine site-specific values to derive numerical coherency functions.

Keywords: spatial variability; coherency model; hard rock site; numerical simulation; plane-wave coherency

Academic Editor: Nikolaos Koukouzas

Received: 22 December 2024
Revised: 5 March 2025
Accepted: 6 March 2025
Published: 7 March 2025

Citation: Lee, D.; Lee, Y.; Kim, H.-S.; Park, J.-S.; Park, D. Sensitivity Analysis of Numerical Coherency Model for Rock Sites. *Appl. Sci.* **2025**, *15*, 2925. https://doi.org/10.3390/app15062925

1. Introduction

When an earthquake occurs, seismic waves do not propagate uniformly through the ground, leading to variations in ground motion even within nearby locations. As a result, the frequency components of seismic waves reaching different points of a structure's foundation may undergo an averaging effect, especially in the high frequency range above 10 Hz [1]. To accurately assess the seismic performance of structures while considering ground motion incoherency, the incoherency Soil–Structure Interaction (SSI) analysis was developed [1,2]. The core element of an incoherency SSI analysis is plane-wave coherency function, which models coherency based on separation distance and frequency by considering the wave passage of seismic waves. Generally, these coherency functions are derived

from empirical data obtained through dense array measurements. The U.S. Nuclear Regulatory Commission (NRC) approved the plane-wave coherency function developed by Abrahamson [1], based on dense array data recorded at the Pinyon Flat site, which is a location that is classified as hard rock [3,4].

The spatial variability of ground motion is primarily influenced by heterogeneity, with ground motion coherency varying based on site-specific conditions [1,3,5–8]. Generally, ground motion coherency is higher in homogeneous and solid geological structures, while it is lower in heterogeneous and weak geological structures. In terms of coherency, soil types (e.g., sand and clay) exhibit lower coherency than rock types (e.g., granite and shale). Existing studies on coherency functions often rely on empirical models that require the installation of dense arrays, resulting in spatial and economic constraints. Moreover, these empirical models may be site-specific and thus cannot be universally applied to all sites with different stratigraphy [9].

Considering the difficulties in developing an empirical coherency function from a site-specific dense array, efforts have been made to utilize numerical simulations for coherency model development. However, these studies have primarily applied idealized conditions. In this study, we use the Pinyon Flat, located in California, as the baseline site. It was selected because it is one of the few sites where a dense array was deployed on a rock profile, from which the empirical coherency function was derived. Additionally, the site has a measured *Vs* profile available. A comprehensive parametric study evaluating the effect of various parameters influencing the calculated coherency function was performed. Systematically analyzing the sensitivity of variables influencing the target output derived from numerical simulations is essential for assessing the reliability of physics-based models and quantitatively evaluating uncertainty [10,11]. We identify which parameters have primary or secondary influences on the calculated coherency and compare the numerically derived function with the site-specific empirical model. Based on the results, we provide guidelines on how to use the numerical model to develop site-specific coherency models.

2. Numerical Coherency Evaluation Methodology

This section outlines the methodology for developing the coherency function from numerical simulations. It also details the procedures for estimating plane-wave coherency and conducting regression analysis to derive the site-specific coherency function.

2.1. Selection of Input Motions

Selecting appropriate input motions is essential for conducting coherency analysis. Svay et al. [5] performed plane-wave coherency analysis using dense seismic array data from Argostoli, Greece. Their study compared plane-wave coherences based on the number of earthquake records used and recommended a minimum of 30 input motions for a stable estimation.

It has been reported that earthquake magnitude has minimal impact on ground motion coherency [3]. Additionally, for evaluating the seismic performance of nuclear power plant structures and equipment in South Korea, the target frequency range typically extends up to 50 Hz. Therefore, when developing coherency functions, earthquake records with a sampling interval of less than 0.01 s are required [12].

To evaluate plane-wave coherency functions using numerical simulations, it is important to select the earthquake records that meet these criteria. In this study, we used 30 input records with a time interval of 0.005 s. Figure 1 shows the distribution of the selected seismic records in terms of epicentral distance, magnitude (M), and peak ground velocity (PGV), which include data from Pacific Earthquake Engineering Research (PEER) database [13] and earthquake records from domestic events in South Korea [14].

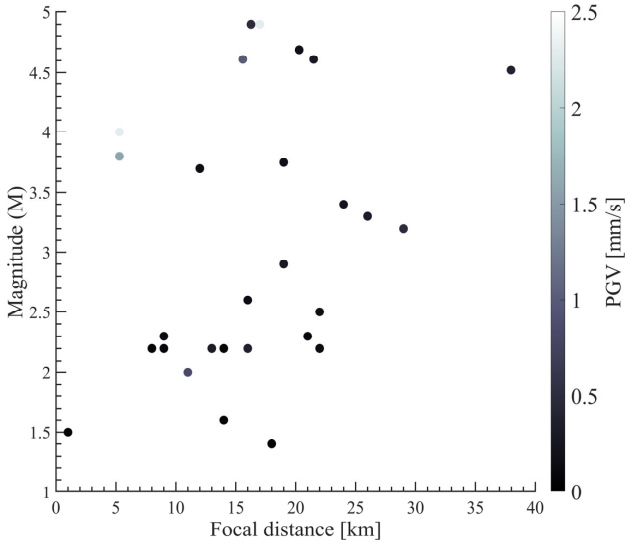

Figure 1. Distribution of selected earthquake records in terms of epicentral distances, M, and PGV.

2.2. Random Field Generation

To simulate the site effect representing the spatial variability of the target site, the Gaussian model was used. MATLAB R2022a, a numerical computation platform for data analysis and algorithm development, was employed to generate the Gaussian random field [15]. For random field generation, the target reference V_s profile is defined, and the CV is calculated using the standard deviation of the obtained V_s profiles. Horizontal and vertical CL are also used as input parameters. The Gaussian random field is generated using these variables and follows a Gaussian correlation function $\rho(\tau)$, which depends on the separation distance τ, as expressed below [16]:

$$\rho_{i,j}(\tau) = exp\left\{-\pi((|\tau|)/CL)^2\right\} \quad (1)$$

The random field was generated using the reference V_s profile, CV profile, and bidirectional CL profile, following a normal probability distribution. In this study, a 2D random field was generated using the reference V_s profile from the Pinyon Flat array [1]. Figure 2 shows the reference V_s profile at the Pinyon Flat array based on down-hole measurements. Figure 3 illustrates an example of the random field generated for the Pinyon Flat array.

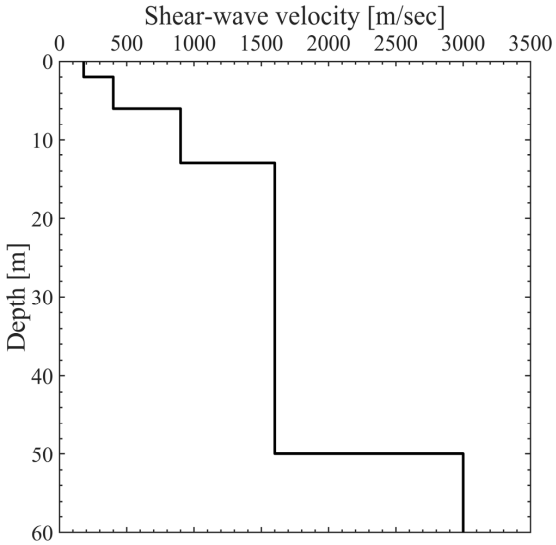

Figure 2. Reference V_s profile at the Pinyon Flat array.

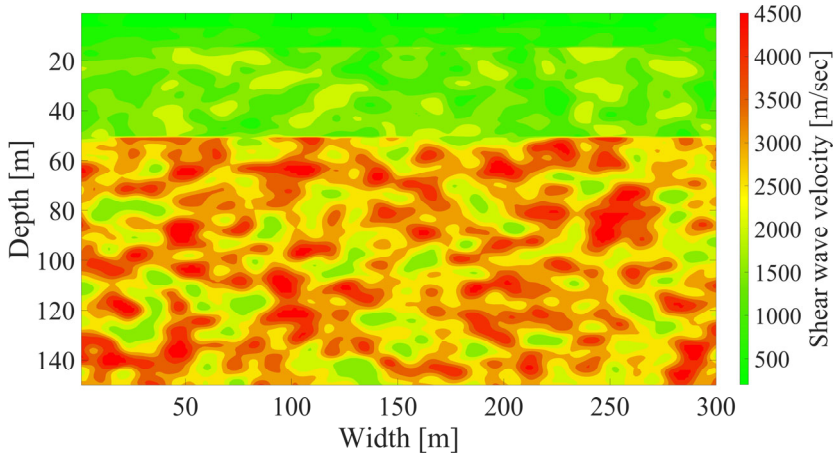

Figure 3. Example realization of random field generated using the Gaussian model for the Pinyon Flat array.

2.3. Numerical Model

The numerical simulation was conducted using OpenSees 3.3.0, a finite element analysis code [17]. The Pinyon Flat site is classified as a hard rock site, characterized by very high stiffness; therefore, the elements were modeled with linear behavior. In time history analysis, boundary conditions and element size significantly influence the results. A viscous damper was applied to the lower boundary to simulate elastic bedrock conditions [18,19]. For the lateral boundaries, the equal degree of freedom (EDOF) method was used to indirectly simulate free-field conditions [20]. To minimize boundary effects, the model width was set to twice the range from which node responses were extracted for coherency analysis.

The element size was determined according to the criteria proposed by Kuhlemeyer and Lysmer [21], ensuring accurate simulation of seismic wave propagation up to the maximum frequency of interest, which was set to 50 Hz. The element size applied was 1 m in both width and height. Figure 4 shows the developed computational model with a depth of 150 m. Because the depth of the numerical model may influence of the calculated coherency, it was changed from 50 m up to 200 m, the results of which are presented in Section 3. The range of nodes used for coherency analysis was defined based on the maximum separation distance of the array installed at the Pinyon Flat site [1].

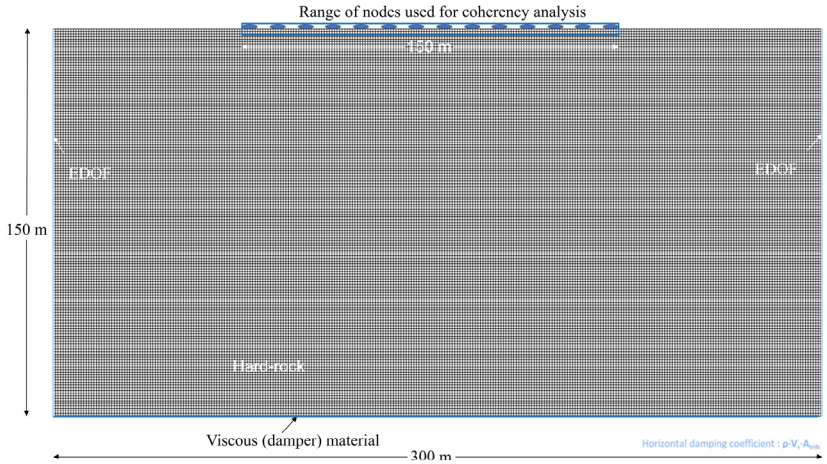

Figure 4. Developed computational model.

2.4. Estimation of Plane-Wave Coherency

We estimated plane-wave coherency following the methodology of Abrahamson [1]. First, the time window for the estimated ground motion is defined. If the time history is too long, it may introduce background noise or affect the Arias intensity. Therefore, a time interval from −10 s to +10 s around the PGV was extracted. To prevent the time window from being too short, the final time window was adjusted by subtracting 0.5 s and adding 1 s to the times corresponding to normalized Arias intensities of 0.1 and 0.75, respectively. The normalized Arias intensity I(τ) at time τ is calculated as follows:

$$I(\tau) = \frac{\int_{T_P-10}^{\tau} \{V_1^2(t) + V_2^2(t)\}dt}{\int_{T_P-10}^{T_P+10} \{V_1^2(t) + V_2^2(t)\}dt} \quad (2)$$

where T_p is the time corresponding to PGV, and V_1 and V_2 are the ground velocities in two horizontal directions, respectively. The endpoints of the extracted time window contain discontinuities that are not zero. Therefore, to prevent abnormal results during the Fourier transform, a 5% cosine-bell taper function is applied to both ends. The taper function is defined as follows:

$$v(t) = \begin{cases} 0.5\left[\cos\left(\frac{t\pi}{0.05W_L} + \pi\right) + 1\right], & t < 0.05W_L \\ 1, & 0.05W_L \le t \le 0.95W_L \\ 0.5\left[\cos\left(\frac{\pi(t-0.95W_L)}{0.05W_L}\right) + 1\right], & t > 0.95W_L \end{cases} \quad (3)$$

where W_L is the length of the final time window, and t is time.

The tapered velocity time history was differentiated to obtain the acceleration time history. Since calculation of coherency is performed in the frequency domain, the discrete Fourier transform was performed using the following equation:

$$u_j(\omega) = \sum_{k=1}^{T} v(t_k)u_j(t_k)e^{-i\omega t_k} \quad (4)$$

where ω is the angular frequency, $u_j(t_k)$ is the acceleration time history at recorded point j, and $v(t_k)$ corresponds to Equation (4).

Seismic coherency analysis is a method for quantifying the similarity between two seismic records. The mathematical definition of seismic coherency involves the smoothed cross-spectrum and smoothed auto-power spectra, which are computed using the following equations:

$$S_{ij}(\omega) = \sum_{m=-M}^{M} a_m u_i(\omega_m)\overline{u_j}(\omega_m) \quad (5)$$

$$S_{ii}(\omega) = \sum_{m=-M}^{M} a_m |u_i(\omega_m)|^2 \quad (6)$$

$$S_{jj}(\omega) = \sum_{m=-M}^{M} a_m |u_j(\omega_m)|^2 \quad (7)$$

where the overbar indicates a complex conjugate, and a_m is the weights used in frequency smoothing, with 2M + 1 indicating the number of smoothed discrete frequencies. A Hamming window of M = 5 was employed, according to Abrahamson [1], and the form is given in Equation (8).

$$\omega(M+1-m) = \omega(m+M+1) = 0.54 + 0.46\cos\left(\frac{\pi m}{M}\right) \quad (8)$$

Plane-wave coherency is estimated as the real part of the complex coherency considering slowness. The complex coherency is defined as the ratio of $S_{ij}(\omega)$ to the geometric mean of $S_{ii}(\omega)$:

$$\gamma_{ij}(\xi_{ij}, \omega) = \frac{S_{ij}(\omega)}{\sqrt{S_{ii}(\omega)S_{jj}(\omega)}} \tag{9}$$

where ξ_{ij} is separation distance between points i and j. The plane-wave coherency is calculated using the following Equation (10):

$$\gamma^{PW}(\xi_{ij}, \omega) = \mathrm{Re}\left[\frac{S_{ij}(\omega)}{\sqrt{S_{ii}(\omega)S_{jj}(\omega)}} e^{-[(d_x)(s_x)+(d_y)(s_y)]\omega i}\right] \tag{10}$$

where d_x and d_y are the separation distances in the x and y directions, respectively, and s_x and s_y are slowness vectors in the x and y directions. Slowness is defined as the reciprocal of the apparent velocity. It is the wave-passage effect that considers the source effect, and plane-wave coherency is equivalent to removing this effect. To consider the source effect in the 2D numerical model, we calculated the plane-wave coherency using the slowness values measured at the Pinyon Flat array. The estimated plane-wave coherency was modeled using the following functional form proposed by Abrahamson [1]:

$$\gamma^{PW}(\xi_{ij}, f) = \left[1 + \left(\frac{f\mathrm{Tanh}(a_3\xi_{ij})}{a_1 f_c(\xi_{ij})}\right)^{n1(\xi_{ij})}\right]^{-1/2} \left[1 + \left(\frac{f\mathrm{Tanh}(a_3\xi_{ij})}{a_2}\right)^{n2}\right]^{-1/2} \tag{11}$$

where a_1, a_2, a_3, n_1, n_2, and f_c are site-specific parameters derived through regression analysis of the calculated plane-wave coherency data. f is frequency. To develop the numerical coherency functions, regression analysis was conducted following the approach of Svay et al. [5]. A nonlinear regression was performed within the frequency range of 1 to 30 Hz, focusing on the site-specific parameters f_c and n_1 in Equation (11), while other parameters were set to the values used in the Pinyon Flat database. This approach was necessary due to convergence issues during the regression process. Consequently, it is important to note that the coherency functions developed in this study are subject to these limitations.

3. Sensitivity Study

In this chapter, the methodology presented in Section 2 is applied to analyze the key parameters influencing plane-wave coherency. The results of the parameter analysis were used to evaluate the reliability of the numerical analysis method by comparing it with the empirically developed coherency model by Abrahamson [1], thereby assessing the performance of the numerical simulations. The key parameters analyzed include the number of numerical analyses, the spatial variability of the site (CV and CL), and the depth of the numerical model. The reference model incorporated the characteristics of the Pinyon Flat site (V_s), which is the target site of Abrahamson's [1] empirical coherency function.

3.1. Numerical of Simulations

Since random fields were used, it is important to select an appropriate number of probabilistic analyses to obtain reasonable results. The number of numerical simulations was determined by the 30 input ground motions and the number of random field realizations. To determine the optimal number of random field realizations, a convergence evaluation was conducted. Figure 5 shows the results of this sensitivity analysis. The results indicate that stable estimates can be achieved when more than 150 analyses are performed up to

the 50 Hz range. Therefore, this study conducted a total of 150 analyses for the coherency evaluation, combining 30 input ground motions with five realizations.

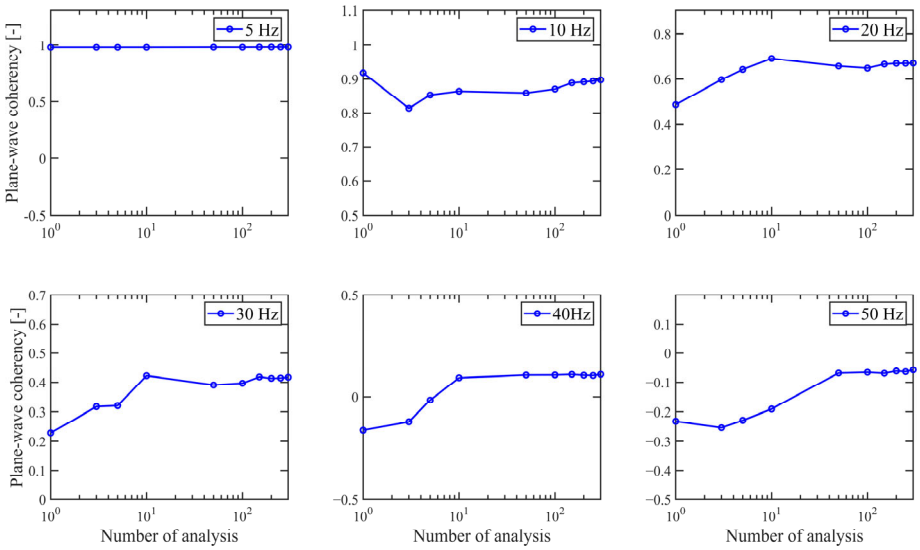

Figure 5. Result of convergence with respect to number of numerical simulations.

3.2. Spatial Variability Parameters

Site-specific coherency has been reported to be highly influenced by spatial variability [1,3,22–24]. We selected the CV and CL, which represent site variability, as sensitivity analysis variables. For the Pinyon Flat site, reference CV and CL profiles were not measured and therefore, are not available. In this study, sensitivity analyses were performed using the range of CV and CL values reported for rock sites [25–27]. The vertical correlation length (CLv) was fixed at 10 m, as recommended in a previous study [23]. Table 1 lists the selected case matrix.

Table 1. Spatial variability and numerical model parameters simulated in this study.

Case Number	CV (%)	CLh (m)	Analysis Depth (m)
Case 1: CV	15, 20, 25, 30	20	150
Case 2: CLh	20	20, 25, 30, 40	150
Case 3: Depth	20	20	50, 100, 150, 200

Figure 6 presents the results of the sensitivity analysis of plane-wave coherency with respect to the CV. The analysis shows that plane-wave coherency decreases as the CV and separation distance increase. This trend is likely due to increased site heterogeneity and seismic wave scattering caused by the spatial variability of V_s and the greater separation distance. This can be interpreted as a decrease in coherency resulting from increased phase differences and interference among individual seismic wave components as the CV increases. Similar patterns have been observed in soil sites with relatively lower stiffness [23]. This suggests that the CV strongly influences coherency regardless of site conditions. Therefore, careful consideration is required when selecting and applying the CV in the development of numerical coherency models for incoherency SSI analysis.

Figure 7 shows the results of the sensitivity analysis of plane-wave coherency with respect to the horizontal correlation length (CLh). Given that the CLh has a greater impact on ground motion coherency than the CLv, the analysis was conducted by fixing the CLv at 10 m and varying the CLh from 20 m to 40 m. The results indicate that the influence of the CLh on plane-wave coherency is minimal as the CLh increases. This suggests that when

the size of the heterogeneity is small relative to the wavelength (i.e., when the CLh is small), the scattering effect of seismic waves due to heterogeneity is reduced, and the influence of separation distance on plane-wave coherency is limited. Especially in the low frequency range, an increase in the CLh has no effect, as the long wavelength seismic components are less influenced. That is, while a larger CLh increases the scale of individual heterogeneities, it does not significantly affect coherency in cases with long wavelengths, such as rock sites. This suggests that when developing numerical coherency models, applying an excessively high CLh value is unlikely to impact coherency.

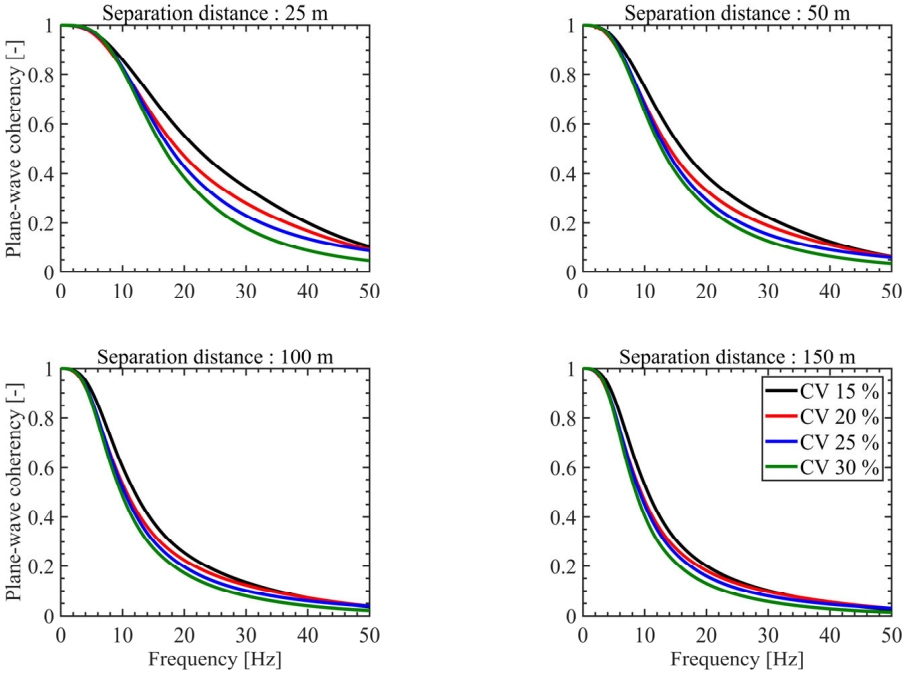

Figure 6. Evaluation of sensitivity analysis regarding effect of CV on plane-wave coherency.

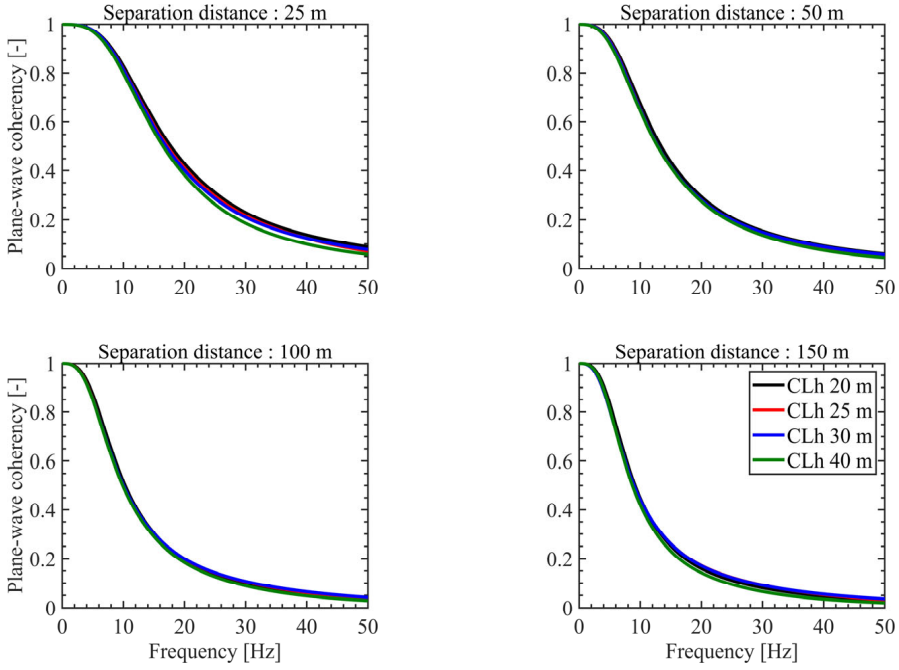

Figure 7. Evaluation of sensitivity analysis regarding effect of CLh on plane-wave coherency.

3.3. Depth of Numerical Model

In numerically deriving the coherency function, the depth of the model may influence the surface variability. However, the effect of the depth of the numerical model has not yet been investigated. To assess its impact on plane-wave coherency, a sensitivity analysis was conducted for depths ranging from 50 m to 200 m. Figure 8 presents the results of the sensitivity analysis with respect to the analysis depth for CV = 20 and CLh = 20. The results indicate that when the analysis depth exceeds 100 m, the calculated coherency converges and that further increases in depth have a marginal influence on the calculated response. This suggests that when the physical properties and spatial variability of the site remain constant, the analysis results converge once the depth exceeds 100 m. However, this result applies only to the Pinyon Flat site. In practice, borehole depth and V_s profile data vary significantly across sites. Therefore, a sensitivity analysis on the depth of the model should be conducted when developing a numerical coherency model.

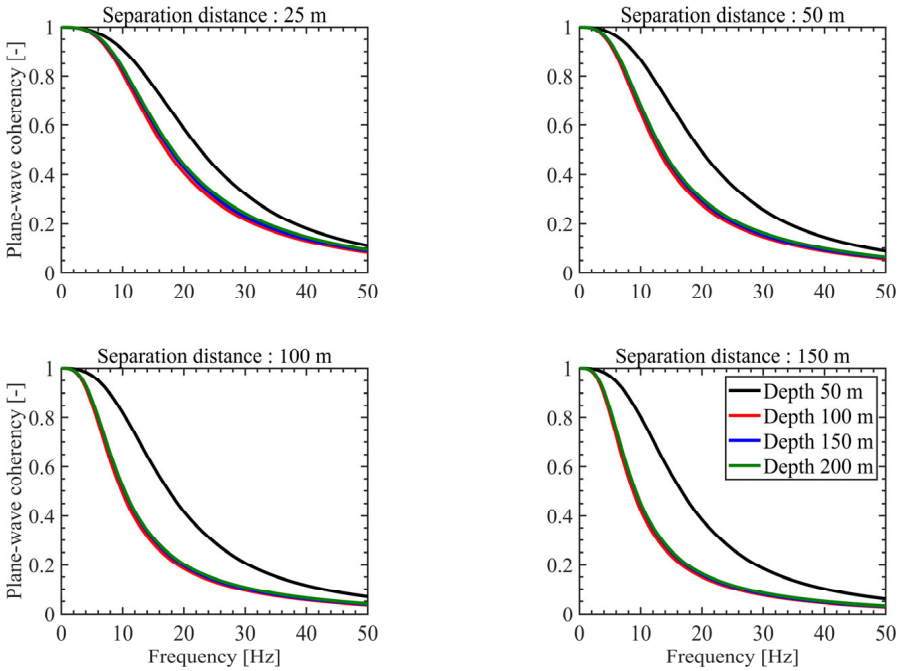

Figure 8. Evaluation of sensitivity analysis regarding effect of analysis depth on plane-wave coherency.

4. Comparison with Empirical Function

Based on the sensitivity analysis results, a comparison was performed with Abrahamson's [1] empirical coherency function. The parameters with minimal impact on plane-wave coherency at hard rock site were fixed as follows: CLv = 10 m, CLh = 20 m, and analysis depth = 150 m. The comparison focused on adjusting the CV, which has the most significant influence on plane-wave coherency. Figure 9 shows the numerical coherency functions derived for the CV range (15–30%) alongside the empirical coherency function. Notably, for CV = 30%, the numerical results closely matched the empirical function across most separation distances and frequency ranges (Table 2). This suggests that if the spatial variability parameters of a target site can be estimated through site investigations, and numerical coherency functions for various hard rock sites can be developed through numerical analysis. However, it is important to note that the results were obtained using spatial variability parameters derived from other hard rock sites, rather than parameters estimated for this target site. Because the spatial variability parameter is inherently site-specific and may differ even within the same rock class, caution is warranted. Further validation of

the numerical functions against empirical functions using spatial variability parameters derived from rigorous site investigations is necessary.

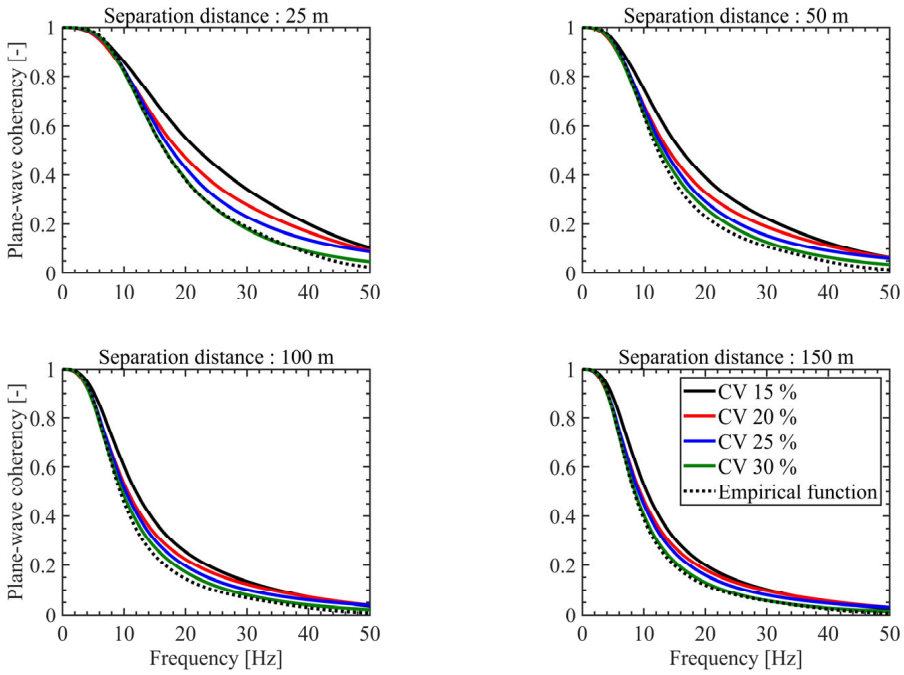

Figure 9. Comparison between numerical-based curve and empirical curve for Pinyon Flat site.

Table 2. R^2 values according to separation distance.

	25 m	**50 m**	**100 m**	**150 m**
R^2 value [-]	0.993	0.985	0.986	0.992

5. Conclusions

This study aimed to analyze the parameters influencing plane-wave coherency at rock sites through a sensitivity analysis based on numerical simulations and to evaluate the reliability of the numerical analysis method by comparing it with empirical coherency functions. The numerical model utilized a 2D Gaussian random field to account for spatial variability. Seismic wave propagation was simulated using the finite element analysis code OpenSees3.3.0.

The sensitivity analysis of four parameters (number of simulations, CV, CL_h, and analysis depth) indicated that 150 simulations are sufficient for stable coherency analysis. The results showed that plane-wave coherency decreases as the CV increases, while the CL_h has a minimal impact. The effect of analysis depth was negligible beyond 100 m. However, since V_s and CV profiles can vary by site, the sensitivity analysis of the analysis depth is recommended when developing numerical coherency functions.

The comparison with the existing empirical coherency function confirmed the reliability of the numerical analysis method. This demonstrates the potential for developing site-specific coherency functions from numerical simulations, which can be widely used for SSI analyses of critical structures, including nuclear power plants and basements linked to tall buildings. The simulation of spatial variable ground motion will help to reduce seismic demand overestimations using uniform motion time histories.

However, several limitations remain. The numerical coherency function requires further validation against empirical results using spatial variability parameters derived from rigorous site investigations. Further studies to enhance the accuracy of the numerically

derived coherency model are warranted, including the utilization of machine learning. The use of probabilistic methods is also recommended to quantify the inherent uncertainty in the coherency estimation.

Author Contributions: Conceptualization, D.P.; methodology, D.L.; software, D.L., Y.L., H.-S.K. and J.-S.P.; formal analysis, D.L., Y.L., H.-S.K. and J.-S.P.; data curation, D.L., Y.L., H.-S.K. and J.-S.P.; writing—original draft preparation, D.L.; writing—review and editing, D.P. and D.L.; supervision, D.P.; funding acquisition, D.P. All authors have read and agreed to the published version of the manuscript.

Funding: This research is funded by National Research Foundation of Korea (NRF) grant funded by the Korean government (MSIT) (No. 2022R1A2C3003245) and Korea Hydro & Nuclear Power Co. Ltd. (No. L24S015000).

Institutional Review Board Statement: Not applicable.

Informed Consent Statement: Not applicable.

Data Availability Statement: The original contributions presented in this study are included in the article. Further inquiries can be directed to the corresponding author.

Conflicts of Interest: Authors Yonghee Lee, Hak-Sung Kim and Jeong-Seon Park were employed by the company Korea Hydro & Nuclear Power Co., Ltd. The remaining authors declare that the research was conducted in the absence of any commercial or financial relationships that could be construed as a potential conflict of interest. The sponsors had no role in the design, execution, interpretation, or writing of the study.

References

1. Abrahamson, N.A. *Hard-Rock Coherency Functions Based on the Pinyon Flat Array Data*; Electric Power Research Institute: Palo Alto, CA, USA, 2007.
2. Kassawara, R. *Validation of CLASSI and SASSI to Treat Seismic Wave Incoherence in SSI Analysis of Nuclear Power Plant Structures*; Electric Power Research Institute: Palo Alto, CA, USA, 2007.
3. Abrahamson, N. *Program on Technology Innovation: Effects of Spatial Incoherence on Seismic Ground Motions*; Electric Power Research Institute: Palo Alto, CA, USA, 2007; p. 1015110.
4. Interim Staff Guidance on Seismic Issues Associated with High Frequency Ground Motion in Design Certification and Combined License Applications. 2008. Available online: https://www.nrc.gov/docs/ML0814/ML081400293.pdf (accessed on 19 May 2008).
5. Svay, A.; Perron, V.; Imtiaz, A.; Zentner, I.; Cottereau, R.; Clouteau1, D.; Bard, P.Y.; Hollender, F.; Lopez-Caballero, F. Spatial coherency analysis of seismic ground motions from a rock site dense array implemented during the Kefalonia 2014 aftershock sequence. *Earthq. Eng. Struct. Dyn.* **2017**, *46*, 1895–1917. [CrossRef]
6. Zerva, A. *Spatial Variation of Seismic Ground Motions: Modeling and Engineering Applications*; CRC Press: Boca Raton, FL, USA, 2016.
7. Zerva, A.; Harada, T. Effect of surface layer stochasticity on seismic ground motion coherence and strain estimates. *Soil Dyn. Earthq. Eng.* **1997**, *16*, 445–457. [CrossRef]
8. Zerva, A.; Zervas, V. Spatial variation of seismic ground motions: An overview. *Appl. Mech. Rev.* **2002**, *55*, 271–297. [CrossRef]
9. Lee, Y.; Lee, D.; Kim, H.-S.; Park, J.-S.; Jung, D.-Y.; Kim, J.; Kim, D.Y.; Lee, Y.; Park, D. Spatial coherency analysis of seismic motions from a hard rock site dense array in Busan, Korea. *Bull. Earthq. Eng.* **2024**, *22*, 7235–7259. [CrossRef]
10. Shi, J.; Li, J.; Li, Y.; Usmani, A.S.; Zhang, L. Numerical investigation of hydrogen vapor cloud explosion from a conceptual offshore hydrogen production platform. *J. Saf. Sustain.* **2024**, *1*, 189–201. [CrossRef]
11. Yan, F.; Xu, K.; Li, D.; Cui, Z. A novel hazard assessment method for biomass gasification stations based on extended set pair analysis. *PLoS ONE* **2017**, *12*, e0185006. [CrossRef] [PubMed]
12. Huerta-Lopez, C.I.; Shin, Y.; Powers, E.J.; Roesset, J.M. Time-frequency analysis of earthquake records. In Proceedings of the 12th World Conference on Earthquake Engineering, Auckland, New Zealand, 30 January–4 February 2000.
13. Ancheta, T.D.; Darragh, R.B.; Stewart, J.P.; Seyhan, E.; Silva, W.J.; Chiou, B.S.-J.; Wooddell, K.E.; Graves, R.W.; Kottke, A.R.; Boore, D.M. NGA-West2 database. *Earthq. Spectra* **2014**, *30*, 989–1005. [CrossRef]
14. Choi, I.; Ahn, J.-K.; Kwak, D. A fundamental study on the database of response history for historical earthquake records on the Korean Peninsula. *KSCE J. Civ. Environ. Eng. Res.* **2019**, *39*, 821–831.
15. Schilling, R.J.; Harris, S.L. *Fundamentals of Digital Signal Processing Using MATLAB: An Instructor's Solutions Manual to Accompany*; Cengage Learning: Boston, MA, USA, 2011.

16. Vanmarcke, E. *Random Fields: Analysis and Synthesis*; MIT Press: Cambridge, MA, USA, 1983.
17. Mazzoni, S.; McKenna, F.; Scott, M.H.; Fenves, G.L. OpenSees command language manual. *Pac. Earthq. Eng. Res. Cent.* **2006**, *264*, 137–158.
18. de la Torre, C.; Bradley, B.; McGann, C. *Assessment of Boundary Conditions for 2D Geotechnical Site-Response Analysis with Soil Heterogeneity*; University of Canterbury: Christchurch, New Zealand, 2021.
19. Pekcan, G.; Mander, J.B.; Chen, S.S. Fundamental considerations for the design of non-linear viscous dampers. *Earthq. Eng. Struct. Dyn.* **1999**, *28*, 1405–1425. [CrossRef]
20. Cook, R.D. *Concepts and Applications of Finite Element Analysis*; John Wiley & Sons: Hoboken, NJ, USA, 2007.
21. Kuhlemeyer, R.L.; Lysmer, J. Finite element method accuracy for wave propagation problems. *J. Soil Mech. Found. Div.* **1973**, *99*, 421–427. [CrossRef]
22. Abbas, H.; Tezcan, J. Analysis and modeling of ground motion coherency at uniform site conditions. *Soil Dyn. Earthq. Eng.* **2020**, *133*, 106124. [CrossRef]
23. Chang, Y.H.; Tsai, C.C.; Ge, L.; Park, D. Influence of horizontally variable soil properties on nonlinear seismic site response and ground motion coherency. *Earthq. Eng. Struct. Dyn.* **2022**, *51*, 704–722. [CrossRef]
24. El Haber, E.; Cornou, C.; Jongmans, D.; Abdelmassih, D.Y.; Lopez-Caballero, F.; Al-Bittar, T. Influence of 2D heterogeneous elastic soil properties on surface ground motion spatial variability. *Soil Dyn. Earthq. Eng.* **2019**, *123*, 75–90. [CrossRef]
25. Nguyen, T.S.; Tanapalungkorn, W.; Likitlersuang, S. Probabilistic analysis of dual circular tunnels in rock masses considering rotated anisotropic random fields. *Comput. Geotech.* **2024**, *170*, 106319. [CrossRef]
26. Jiang, S.; Li, D.; Zhou, C.; Phoon, K. Slope reliability analysis considering effect of autocorrelation functions. *Chin. J. Geotech. Eng.* **2014**, *36*, 508–518.
27. Zhang, Q.; Wang, L.; Zhang, H. Rainfall infiltration process of a rock slope with considering the heterogeneity of saturated hydraulic conductivity. *Front. Earth Sci.* **2022**, *9*, 804005. [CrossRef]